Inorganica Chimica Acta 434 (2015) 113–120

Contents lists available at ScienceDirect

Inorganica Chimica Acta

journal homepage: www.elsevier.com/locate/ica

Synthesis, crystal structures and catalytic activity of tetrakis(acetato)dirhodium(II) complexes with axial picoline ligands

Qing-Song Ye [a,b], Xiao-Nian Li [c], Yi Jin [d,*], Juan Yu [b], Qiao-Wen Chang [b], Jing Jiang [b], Cai-Xian Yan [b], Jie Li [b], Wei-Ping Liu [a,b,*]

[a] School of Material Science and Engineering, Kunming University of Science and Technology, Kunming 650093, China
[b] State Key Lab of Advanced Technologies for PGM, Kunming Institute of Precious Metals, Kunming 650106, China
[c] Analysis and Test Center, State Key Laboratory of Phytochemistry and Plant Resources in West China, Kunming Institute of Botany, Chinese Academy of Sciences, Kunming 650201, China
[d] Key Laboratory of Medicinal Chemistry for Natural Resource, Ministry of Education, School of Chemical Science and Technology, Yunnan University, Kunming 650091, China

ARTICLE INFO

Article history:
Received 27 December 2014
Received in revised form 9 May 2015
Accepted 15 May 2015

Keywords:
Rhodium
Acetate
Picoline
Catalytic activity
C–H···O hydrogen bond
Axial ligand

ABSTRACT

Three complexes were synthesized in high yields by reaction of $Rh_2(O_2CCH_3)_4$ with 2-picoline (**1**), 3-picoline (**2**) and 4-picoline (**3**), respectively, and characterized by elemental analysis, ESI^+-MS, FT-IR and ^1H NMR along with single-crystal X-ray structural analysis. All picoline ligands coordinate to the axial sites of $Rh_2(O_2CCH_3)_4$ via the pyridine nitrogen atoms, and interestingly, the coordination of 2-picoline in **1** is assisted by two intramolecular C–H···O hydrogen bonds formed between the methyl of 2-picoline and the oxygen atoms of $Rh_2(O_2CCH_3)_4$. Moreover, the intermolecular C–H···O interactions play the main role in the structural stacking of **1**–**3**. Their catalytic activity was evaluated in the C–H insertion reactions for the preparation of 4-nitrobenzyl-(4R,5R,6S)-6-((R)-1-hydroxyethyl)-4-methyl-3,7-dioxo-1-azabicyclo [3.2.0] heptane-2-carboxylate, a key intermediate of Meropenem. The isolated yields for **1**, **2** and **3** are 44%, 16% and 22%, respectively, significantly lower than the value of $Rh_2(O_2CCH_3)_4$ (73%), indicating that the axial ligands have negative but different influence on the catalytic activity. The activities of **1**–**3** are related to the displacement rate of the axial ligands, and essentially related to the Rh–N bond lengths which strong affect the displacement rate. Therefore, it is possible to tune the catalytic activity of $Rh_2(O_2CCH_3)_4$ by changing its axial ligands.

1. Introduction

Dirhodium(II) tetracarboxylates of type $Rh_2(O_2CR)_4L_2$, in which the four carboxylates (the equatorial ligands) bridge the two rhodium atoms and L represents a Lewis base (the axial ligands) bound to the Rh–Rh axis, have attracted considerable attention in recent years due to their potential applications as catalysts [1–6], antitumor agents [7–13] and building blocks for supramolecular arrays [14–16]. Dirhodium(II) tetracarboxylates are quite stable and can be used to construct various new derivatives via equatorial ligand substitution or axial ligand exchange [16,17]. The equatorial ligand substitution usually takes place at reflux in high boiling-point solvents, while the axial ligand exchange reaction can quickly occur at room temperature. This different reactivity resulted in the isolation of several dirhodium(II) tetracarboxylates and large amounts of axial adducts [16–18]. Among these adducts, the axial ligands are mostly nitrogenous heterocyclic compounds. Typical examples of this type of ligands are pyridine and its derivatives. The adducts, formed by reaction of pyridine and its derivatives with dirhodium(II) tetracarboxylates, have been extensively investigated since the discovery the paddlewheel structure of dirhodium(II) tetraacetate [17,18]. However, it is surprising that the picoline adducts of dirhodium(II) tetracarboxylates have not been systemically explored up to now, although picoline is an obvious derivative of pyridine. In this context, we report the characterization, crystal structures and catalytic activity of three picoline adducts of dirhodium(II) tetraacetate.

2. Experimental

2.1. General

Tetrakis(acetato)dirhodium(II) ($Rh_2(O_2CCH_3)_4$) was prepared using literature procedure [19]. (3S,4R)-3-[(1R)-1-Hydroxyethyl]-

* Corresponding authors at: School of Material Science and Engineering, Kunming University of Science and Technology, Kunming 650093, China (W.-P. Liu). Tel./fax: +86 871 6832 9899.
E-mail addresses: jinyi@ynu.edu.cn (Y. Jin), liuweiping0917@126.com (W.-P. Liu).

http://dx.doi.org/10.1016/j.ica.2015.05.017
0020-1693/

Table 1
Crystal data and structural refinements for **1**–**3**.

	1	**2**	**3**
Empirical formula	$C_{20}H_{26}N_2O_8Rh_2$	$C_{20}H_{26}N_2O_8Rh_2$	$C_{20}H_{26}N_2O_8Rh_2$
M_r	628.25	628.25	628.25
T (K)	100(2)	100(2)	100(2)
λ (Å)	0.71073	0.71073	0.71073
Crystal system	monoclinic	triclinic	monoclinic
Space group	$P2_1/c$	$P\bar{1}$	$P2_1/c$
a (Å)	7.6476(12)	7.7224(8)	10.4429(13)
b (Å)	19.930(3)	8.2418(9)	12.9252(16)
c (Å)	8.2011(13)	10.6156(11)	8.8736(11)
α (°)	90	77.661(1)	90
β (°)	115.963(2)	71.673(1)	101.897(2)
γ (°)	90	62.427(1)	90
V (Å^3)	1123.8(3)	566.66(10)	1172.0(3)
Z	2	1	2
D_{calc} (g cm^{-3})	1.857	1.841	1.780
μ (mm^{-1})	1.517	1.505	1.455
F(000)	628	314	628
Crystal size (mm^3)	0.28 × 0.09 × 0.04	0.23 × 0.20 × 0.04	0.13 × 0.13 × 0.06
θ range (°)	2.04–27.99	2.03–27.99	1.99–28.00
Limiting indices	$-10 \leqslant h \leqslant 10$, $-26 \leqslant k \leqslant 25$, $-10 \leqslant l \leqslant 10$	$-10 \leqslant h \leqslant 10$, $-10 \leqslant k \leqslant 10$, $-14 \leqslant l \leqslant 13$	$-13 \leqslant h \leqslant 13$, $-17 \leqslant k \leqslant 17$, $-11 \leqslant l \leqslant 11$
Reflection collected	10,657	7351	11,286
Independent reflection (R_{int})	2704 (0.0410)	2707 (0.0243)	2816 (0.0494)
Max. and min. transmission	0.9418 and 0.6760	0.9423 and 0.7235	0.9178 and 0.8334
Data/restraints/parameters	2704/0/146	2707/0/233	2816/0/148
Goodness-of-fit (GOF) on F^2	1.048	1.071	1.014
Final R indices [$I > 2\sigma(I)$]	R_1 = 0.0312, wR_2 = 0.0650	R_1 = 0.0243, wR_2 = 0.0598	R_1 = 0.0300, wR_2 = 0.0644
R indices (all data)	R_1 = 0.0449, wR_2 = 0.0692	R_1 = 0.0284, wR_2 = 0.0621	R_1 = 0.0504, wR_2 = 0.0709
$\Delta\rho_{max/min}$ (e Å^{-3})	1.008/−0.838	0.586/−1.270	0.762/−0.650

4-[(1R)-1-methyl-3-diazo-3-(*p*-nitrobenzyloxycarbonyl)-2-oxo-propyl]azetidin-2-one (**4**) was purchased from Sigma–Aldrich Co. Ltd. All chemicals and solvents were used as received without further purification, unless otherwise stated. Elemental analyses for C, H and N were performed with a Carlo-Erba Instrument. Electrospray ionization mass spectra (ESI-MS) studies were carried out on an Agilent G6230 Spectrometer. FT-IR spectra were recorded in the 4000–400 cm^{-1} region on a Bruker Tensor 27 Spectrometer with KBr pellets. ^{1}H and ^{13}C NMR spectra were obtained on a Bruker Avance 400 spectrometer with TMS as an internal standard. Melting points were determined on a Thomas Hoover capillary melting point apparatus and were uncorrected. Optical rotations were measured with a Perkin–Elmer 240 polarimeter. UV–Vis spectra were recorded on a Varian Cary 50 spectrophotometer equipped with a PCB-150 water circulator. Column chromatography was performed on silica gel (200–300 mesh).

2.2. Synthesis

Complexes **1**–**3** were prepared by a similar procedure. In general, an aqueous solution (30 mL) of $Rh_2(O_2CCH_3)_4$ (0.031 g, 0.07 mmol) was placed in a Schlenk tube. After an ethanol aqueous solution (1:1 v/v, 10 mL) was carefully layered on the previous solution as a middle layer, an ethanol solution (10 mL) of picoline (0.052 g, 0.56 mmol) was put onto the layer. The tube was left undisturbed for one week to yield pink single crystals. The crystals were collected on a frit, washed with water and ethanol, and dried in vacuo.

2.2.1. $Rh_2(O_2CCH_3)_4(2\text{-}CH_3\text{-}C_5H_4N)_2$ (**1**)

Yield: 41 mg (93%). *Anal.* Calc. for $C_{20}H_{26}N_2O_8Rh_2$: C, 38.24; H, 4.17; N, 4.46. Found: C, 38.0; H, 4.1; N, 4.4%. ESI$^+$-MS (in MeOH) m/z: 465, [M − 2Picoline + Na]$^+$; 506, [M − 2Picoline + 2CH$_3$OH]$^+$; 907, [2 M − 4Picoline + Na]$^+$. IR (KBr): 3026 (w), 2988 (w), 2935 (w), 1593 (vs), 1486 (m), 1434 (vs), 1345(m), 1308(m), 772 (m), 699 (s). ^{1}H NMR (400 MHz, DMSO-d_6) δ 8.49 (br s, 2H, Py-*H*), 7.71 (br s, 2H, Py-*H*), 7.24 (br, 4H, Py-*H*), 2.49 (s, Py-*CH*$_3$, overlapped with the methyl of DMSO), 1.79 (s, 12H, 4*CH*$_3$COO).

2.2.2. $Rh_2(O_2CCH_3)_4(3\text{-}CH_3\text{-}C_5H_4N)_2$ (**2**)

Yield: 40 mg (91%). *Anal.* Calc. for $C_{20}H_{26}N_2O_8Rh_2$: C, 38.24; H, 4.17; N, 4.46. Found: C, 38.2; H, 4.1; N, 4.3%. ESI$^+$-MS (in MeOH) m/z: 465, [M − 2Picoline + Na]$^+$; 506, [M − 2Picoline + 2CH$_3$OH]$^+$; 558, [M − Picoline + Na]$^+$; 907, [2 M − 4Picoline + Na]$^+$; 1000, [2 M − 3Picoline + Na]$^+$. IR (KBr): 3017 (w), 2983 (w), 2928 (w), 1591 (vs), 1481 (m), 1433 (vs), 1345 (m), 792 (m), 706 (s). ^{1}H NMR (400 MHz, DMSO-d_6) δ 8.94 (br, 2H, Py-*H*), 8.42 (br, 2H, Py-*H*), 7.63 (br, 2H, Py-*H*), 7.32 (br, 2H, Py-*H*), 2.32 (s, Py-*CH*$_3$, partially overlapped with the methyl of DMSO), 1.77 (s, 12H, 4*CH*$_3$COO).

2.2.3. $Rh_2(O_2CCH_3)_4(4\text{-}CH_3\text{-}C_5H_4N)_2$ (**3**)

Yield: 41 mg (93%). *Anal.* Calc. for $C_{20}H_{26}N_2O_8Rh_2$: C, 38.24; H, 4.17; N, 4.46. Found: C, 37.9 H, 4.1; N, 4.4%. ESI$^+$-MS (in MeOH) m/z: 465, [M − 2Picoline + Na]$^+$; 506, [M − 2Picoline + 2CH$_3$OH]$^+$; 558, [M − Picoline + Na]$^+$; 599, [M − Picoline + 2CH$_3$OH]$^+$; 907, [2 M − 4Picoline + Na]$^+$; 1000, [2 M − 3Picoline + Na]$^+$; 1093, [2 M − 2Picoline + Na]$^+$. IR (KBr): 3013 (w), 2985 (w), 2921 (w), 1592 (vs), 1498 (m), 1432 (vs), 1348 (m), 818 (m), 697 (s). ^{1}H NMR (400 MHz, DMSO-d_6) δ 8.44 (br, 4H, Py-*H*), 7.21 (br s, 4H, Py-*H*), 2.32 (s, Py-*CH*$_3$, partially overlapped with the methyl of DMSO), 1.77 (s, 12H, 4*CH*$_3$COO).

2.3. Preparation the sample solutions for UV–Vis analysis

UV–Vis signals of **1**–**3** in the range 350–700 nm were recorded in three solvents, dimethyl sulfoxide (DMSO), methanol and ethyl acetate. For the DMSO solutions, each complex (10 mg, for **1**, **2**, **3** or $Rh_2(O_2CCH_3)_4$) was suspended in 10 mL of DMSO, then the resulting mixtures were stirred at room temperature. Complex **1**

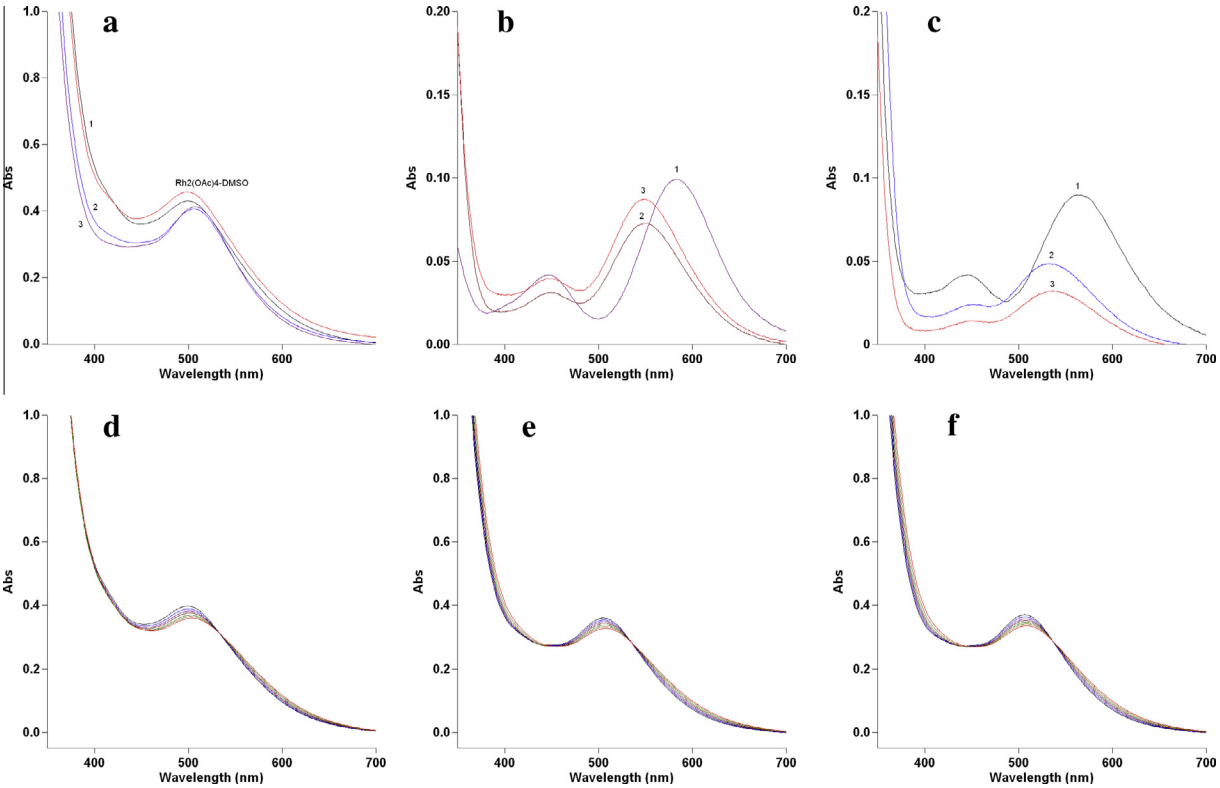

Fig. 1. UV–Vis analysis of complexes **1**–**3** in different solutes: (a) in DMSO; (b) in methanol; (c) in ethyl acetate; UV–Vis analysis of complexes **1**–**3** in DMSO from 20 to 50 °C: (d) complex **1**; (e) complex **2**; (f) complex **3**.

and $Rh_2(O_2CCH_3)_4$ were quickly dissolved within 30 min, but **2** and **3** were dissolved within 5 h. For the methanol and ethyl acetate solutions, each complex (5 mg, for **1**, **2** or **3**) was added to two different solvents (15 ml), methanol or ethyl acetate, respectively. Then these mixtures were stirred for 24 h at room temperature. Complex **1** was completely dissolved in the both solvents, and the color of solutions was changed to light blue, different from the purple color of free complex **1**. Complexes **2** and **3**, however, were only partially dissolved in the both solvents, and the colors of solutions were light purple same as the purple color of free complexes **2** or **3**. All solution samples have been filtered by filtration membranes (PTFE, ϕ = 0.45 μm) prior to test for UV–Vis analysis. Meanwhile, the solutions of complexes **1**–**3** in DMSO were analyzed by UV–Vis at different temperature from 20 to 50 °C.

2.4. Single crystal X-ray data collection and structure determination

Single crystals of **1**–**3** were obtained as described above. Intensity data for single crystals of each complex were collected on a BRUKER SMART APEX II CCD detector with graphite-monochromatized Mo Kα radiation (λ = 0.071073 nm). The structures were solved by direct method using the program SHELXS-97 and subsequent Fourier difference techniques, and refined anisotropically by full matrix least-squares on F^2 using SHELXL-97 [20]. Crystal data and structural refinements of **1**–**3** are shown in Table 1.

2.5. Evaluation of catalytic activity

Complexes **1**–**3** and dirhodium(II) tetraacetate were used as catalysts for the preparation of 4-nitrobenzyl-(4R,5R,6S)-6-((R)-1-hydroxyethyl)-4-methyl-3,7-dioxo-1-azabicyclo [3.2.0] heptane-2-carboxylate (**5**). The general preparation method was described as below. Firstly, four different catalysts of complexes **1**, **2**, **3** and $Rh_2(O_2CCH_3)_4$ (1 mg, 5 mg or 10 mg, respectively) were added to 10 ml of ethyl acetate, and stirred for 1 h at room temperature. Because of the low solubilities of complexes **2** or **3** in ethyl acetate, which are only partially dissolved, all mixed solutions were filtered by filtration membranes (PTFE, ϕ = 0.45 μm). Then, these filtrates were immediately added to the solution of compound **4** (500 mg, 1.28 mmol) and 10 ml of ethyl acetate in a 25-ml round-bottomed flask, respectively. The result solutions were heated to reflux, gas evolution occurred. After refluxing for 15 min, the mixture was evaporated in vacuo to give crude product as foams and purified by flash column chromatography (Petroleum ether: Ethyl acetate = 1: 1) to yield compound **5**. Each sample was measured in parallel for three trials.

2.5.1. (3S,4R)-3-[(1R)-1-Hydroxyethyl]-4-[(1R)-1-methyl-3-diazo-3-(p-nitrobenzyloxycarbonyl)-2-oxopropyl]azetidin-2-one (**4**)

Melting Point = 115–117 °C; ^{1}H NMR (400 MHz, $CDCl_3$): δ 1.17 (d, J = 6.8 Hz, 3H, 1-β-methyl), 1.24 (d, J = 6.4 Hz, 3H, CH_3CHOH), 2.85 (d, J = 4.8 Hz, 1H, H3), 3.16 (s, 1H, *OH*), 3.71 (q, J = 6.4 Hz, 1H, *CH*CH_3), 3.82 (t, J = 4.4 Hz, 1H, H4), 4.08 (t, J = 5.6 Hz, 1H, *CH*OH), 5.34 (s, 2H, CO_2CH_2), 6.65 (s, 1H, *NH*), 7.51 and 8.22 (d, J = 8.4 Hz, 2H, aromatic protons); ^{13}C NMR (125 MHz, $CDCl_3$): δ 13.41 (1-β-methyl), 21.03 (CH_3CHOH), 45.02 (C6), 53.21 (C4), 61.95 (C3), 65.48 (*CH*OH), 65.68 (CO_2CH_2), 124.02 (aromatic carbons), 128.78 (aromatic carbons), 141.94 (2C, aromatic carbon), 147.98 (C8), 160.43 (CO), 168.271 (CO), 194.78 (CO); IR (KI, film) 2140, 1750, 1720 and 1650 cm^{-1}; $[\alpha]_D^{21}$ = −50.6° (c = 2.5, CH_2Cl_2); ESI$^+$-MS (in MeOH) m/z: $[M + Na]^+$ Calcd. for $C_{17}H_{18}N_4O_7Na$ 413.1073; Found 413.1067. The ^{1}H NMR of compound **4** is consistent with the reported values in the literature [21]. (^{1}H NMR ($CDCl_3$): δ 1.22 (d, J = 6.0 Hz, 3H, 1-β-methyl), 1.32 (d, J = 6.0 Hz, 3H, CH_3CHOH), 2.38 (d, J = 3.2 Hz, 1H, *OH*), 2.92 (dd, J = 2.4 and

Table 2
Selected bond lengths (Å) and angles (°) for **1**.

Rh1–O1	2.051(2)	Rh1–O2	2.039(2)
Rh1–O3	2.042(2)	Rh1–O4A	2.045(2)
Rh1–N1	2.317(3)	Rh1–Rh1A	2.4121(5)
O1–Rh1–O3	90.58(9)	O1–Rh1–O4A	90.14(9)
O2–Rh1–O3	88.78(9)	O2–Rh1–O4A	90.14(9)
O1–Rh1–O2	175.49(9)	O3–Rh1–O4A	175.38(9)
N1–Rh1–Rh1A	176.42(7)		

Symmetry code: A: $-x+1, -y+1, -z+2$.

Table 3
Selected bond lengths (Å) and angles (°) for **2**.

Rh1–O1	2.027(3)	Rh1–O2A	2.018(3)
Rh1–O3A	2.038(2)	Rh1–O4	2.048(2)
Rh1–N1	2.260(5)	Rh1–N1′	2.252(5)
Rh1–Rh1A	2.3837(4)		
O1–Rh1–O3A	90.18(9)	O1–Rh1–O4	89.60(9)
O2A–Rh1–O3A	89.80(9)	O2–Rh1–O4	90.14(9)
O1–Rh1–O2A	176.15(13)	O3A–Rh1–O4A	175.90(6)
N1–Rh1–Rh1A	170.30(15)	N1′–Rh1–Rh1A	168.87(15)

Symmetry code: A: $-x+2, -y+2, -z+1$.

Table 4
Selected bond lengths (Å) and angles (°) for **3**.

Rh1–O1	2.033(2)	Rh1–O2	2.045(2)
Rh1–O3	2.031(2)	Rh1–O4	2.043(2)
Rh1–N1	2.247(3)	Rh1–Rh1A	2.4010(5)
O1–Rh1–O3	89.96(9)	O1–Rh1–O4	89.95(10)
O2–Rh1–O3	89.76(10)	O2–Rh1–O4	90.02(10)
O1–Rh1–O2	175.84(8)	O3–Rh1–O4	175.82(9)
N1–Rh1–Rh1A	178.08(7)		

Symmetry code: A: $-x, -y, -z+2$.

7.6 Hz, 1H, H3), 3.77 (q, J = 6.0 Hz, 1H, *CH*CH_3), 3.86 (dd, J = 2.4 and 6.0 Hz, 1H, H4), 4.15 (m, 1H, *CH*OH), 5.38 (s, 2H, CO_2CH_2), 5.90 (s, 1H, *NH*), 7.57 and 8.30 (d, J = 6.6 Hz, 2H, aromatic protons)).

*2.5.2. 4-nitrobenzyl-(4R,5R,6S)-6-((R)-1-hydroxyethyl)-4-methyl-3,7-dioxo-1-azabicyclo [3.2.0] heptane-2-carboxylate (**5**)*

Melting Point = 125–127 °C; ^{1}H NMR (400 MHz, $CDCl_3$): δ 1.19 (d, J = 6.8 Hz, 3H, 1-β-methyl), 1.34 (d, J = 6.4 Hz, 3H, CH_3CHOH), 2.82 (m, 1H, *CH*CH_3), 3.27 (d, J = 6.8 Hz, 1H, H6), 4.23 (d, J = 6.8 Hz, 1H, H5), 4.31 (m, 1H, *CH*OH), 4.47 (s, 1H, H2), 5.33–5.22 (dd, J = 13.6 Hz, 2H, CO_2CH_2), 8.20 and 7.51 (d, J = 8.4 Hz, 2H, aromatic protons); ^{13}C NMR (125 MHz, $CDCl_3$): δ 12.62 (1-β-methyl), 21.92 (CH_3CHOH), 41.96 (C4), 55.57 (C5), 61.69 (C6), 62.05 (C2), 65.64 (*CH*OH), 66.27 (CO_2CH_2), 123.90 (aromatic carbons), 128.34 (aromatic carbons), 141.94 (aromatic carbon), 147.85 (aromatic carbon), 164.95 (CO), 172.70 (CO), 208.88 (CO); IR (KI, film) 1780, 1745 and 1605 cm^{-1}; $[\alpha]_D^{21}$ = +43.3° (c = 2.5, CH_2Cl_2); ESI$^+$-MS (in MeOH) m/z: $[M+Na]^+$ Calcd. for $C_{17}H_{18}N_2O_7Na$ 385.1012; Found 385.1006. The ^{1}H NMR of compound **5** is consistent with the reported values in the literature [22]. (^{1}H NMR ($CDCl_3$): δ 1.18 (d, J = 6.2 Hz, 3H, CH_3), 1.28 (d, J = 6.1 Hz, 3H, CH_3), 2.96 (m, 1H, CH), 3.12 (m, 1H, CH), 3.98 (m, 1H, CH), 4.00 (m, 1H, CH), 4.56 (s, 1H, CH), 4.86–5.02 (m, 2H, CH2), 7.69 (d, J = 8.7 Hz, Ar–H), 8.25 (d, J = 8.6 Hz, 2H, Ar–H).

3. Results and discussion

Complexes **1**–**3** were synthesized by the direct reaction of $Rh_2(O_2CCH_3)_4$ with an excessive amounts of the picoline ligands. The reactions were essentially quantitative to afford high isolated yields (91–93%). The complexes are insoluble in common solvents, but slightly soluble in strong donor solvents such as dimethyl sulfoxide (DMSO) or pyridine.

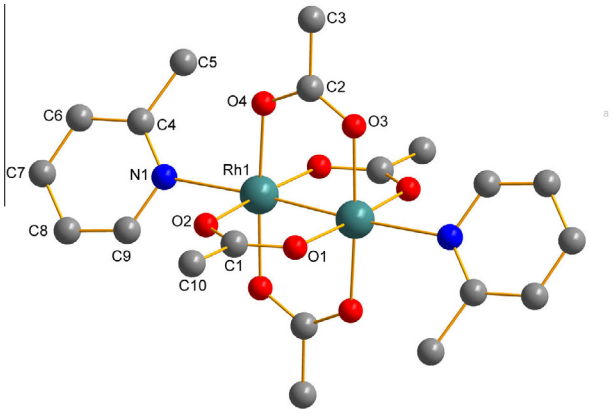

Fig. 2. A view of the molecule structure of **1** with the atomic labeling scheme. Hydrogen atoms were omitted for clarity.

All complexes were characterized by elemental analysis, FT-IR, ESI$^+$-MS and ^{1}H NMR. The elemental analysis data are in good agreement with the calculated values. In all three complexes, the symmetric and asymmetric stretching vibration bands of the acetate ligands, observed as strong intensity bands at 1432–1434 cm^{-1} and 1591–1593 cm^{-1}, respectively, are essentially equal. The values of the difference between ν_{asym}(COO) and ν_{sym}(COO), as expected, are less than 200 cm^{-1} ($\Delta\nu$ = 158–160 cm^{-1}), consistent with a bidentate bridging mode for the acetates [23]. These IR data agree well with those observed in dimeric rhodium complexes of other alkyl carboxylates, in which the carboxylate acts as a bridging bidentate ligand [18].

Complex **1** shows two peaks at m/z 465 and 506 which can be assigned to the fragment $[M-2Picoline+Na]^+$ and $[M-2Picoline+2CH_3OH]^+$, respectively. Interestingly, **1** develops a peak at m/z 907, due to the loss of four picoline residues from two molecules of **1** accompanied by the gain of one sodium cation. Besides the three peaks observed in **1**, **2** shows two more peaks at m/z 558 and 1000, corresponding to $[M-Picoline+Na]^+$ and $[2M-3Picoline+Na]^+$, respectively. The former was attributed to a loss of one picoline molecule accompanied by the gain of one Na^+, while the latter was formed by the same procedure as the peak at m/z 907 except for the loss of three picoline residues. As compared to **2**, two more peaks, at m/z 599 and 1093, are observed in **3**, and they are assigned to $[M-Picoline+2CH_3OH]^+$ and $[2M-2Picoline+Na]^+$, respectively. It is noteworthy that no complexes show M^+ peaks, presumably due to the low stability of their axial ligands under electron spray ionization, which are

Table 5
Selected bond lengths in the $Rh_2(O_2CCH_3)_4L_2$ adducts, where L = py, 2-mpy, ampy, dmp, aamp, 4-mpy and pym.[a]

L	Rh–Rh (Å)	Rh–N (Å)	Ref.
py	2.3963(2)	2.227(3)	
2-mpy	2.4121(5)	2.317(3)	This work
ampy[b]	2.417(3)	2.36(1)	
dmpy	2.4137(5)	2.403(4)	
aampy	2.4112(6)	2.439(4)	
4-mpy	2.4010(5)	2.247(3)	This work
pym	2.4030(7)	2.243(3)	

[a] py, 2-mpy, ampy, dmpy, aampy, 4-mpy and pym denote pyridine, 2-picoline, 2-amino-6-methylpyridine, 2,6-dimethylpyridine, 2-acetylamino-6-methylpyridine, 4-picoline, 4-pyridinemethanol.
[b] The values are the complex where the two axial sites of the dirhodium unit are occupied with pyridine.

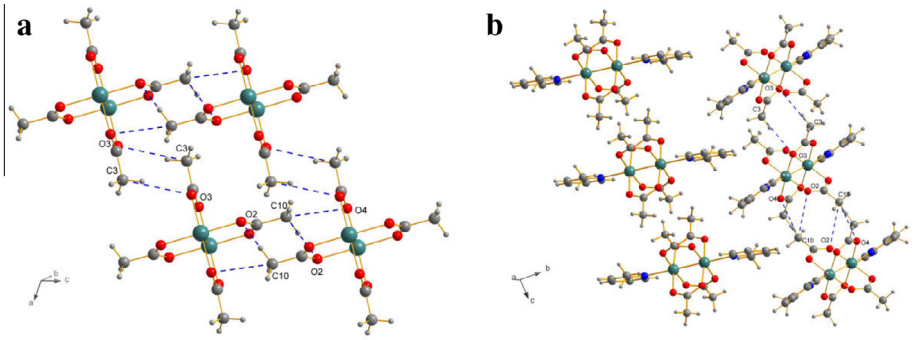

Fig. 3. (a) A portion of the sheet in **1** formed by C–H···O hydrogen bonds of C3···O3 (3.448(5) Å), C10···O2 (3.378(5)···Å) and C10···O4 (3.500(6) Å). The axial 2-picoline ligands were omitted for clarity. (b) The crystal packing of molecules **1**.

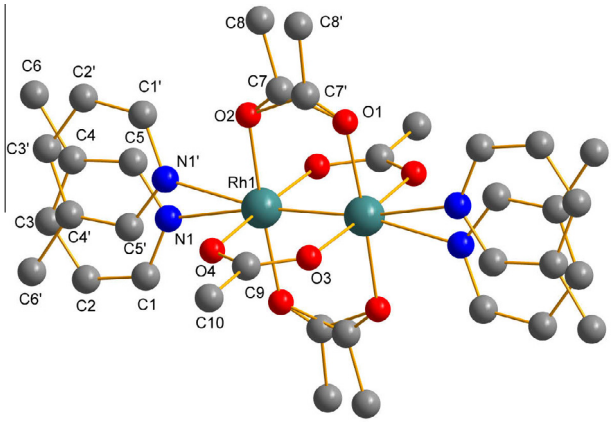

Fig. 4. A view of the molecule structure of **2** with the atomic labeling scheme. Hydrogen atoms were omitted for clarity.

consistent with our previous observation for bis(pyridine) adducts of dirhodium tetraoctanoate [24].

The UV–Vis spectra of **1**–**3** in three different solvents are showed in Fig. 1(a–c). The max absorption peaks of **1**–**3** in DMSO (Fig 1a) are almost the same (498.2, 503.1 505.5 nm for **1**, **2**, **3**, respectively) and they are also same as $Rh_2(O_2CCH_3)_4(DMSO)_2$ (λ_{max} = 498.0 nm) which is directly prepared by dissolving $Rh_2(O_2CCH_3)_4$ in DMSO. This result shows that **1**–**3** are unstable and may be converted to $Rh_2(O_2CCH_3)_4(DMSO)_2$ in DMSO solution, further evidence for which is provided by that the absorption curves of **1**–**3** in DMSO are almost no change from 20 to 50 °C (Fig 1d–f). Compared to the almost same absorption curves of **1**–**3** in DMSO, the λ_{max} of **1** in methanol (584.9 nm) is very different from the values of **2** and **3** (549.0 nm and 547.0 nm for **2** and 3, respectively, Fig. 1b). This result may be explained by their different stability in methanol. Complex **1** is also unstable and maybe completely turned to be $Rh_2(O_2CCH_3)_4(methanol)_2$ in methanol. Complexes **2** and **3** are partially stabilization, and they could be solvated to be the $Rh_2(O_2CCH_3)_4$(methanol)(picoline) or mixture of $Rh_2(O_2CCH_3)_4(methanol)_2$ and $Rh_2(O_2CCH_3)_4$ (methanol)(picoline). These are consistent with the ESI-MS results, for **1**, there are fragment $[M - 2Picoline + 2Na \text{ (or } 2Solvent)]^+$, but not found fragment $[M - Picoline + Na \text{ (or Solvent)}]^+$. However, for **2** and **3**, fragment $[M - Picoline + Na \text{ (or Solvent)}]^+$ can be found. In ethyl acetate, similar absorption spectra to methanol were observed except that the maximum absorptions were blue-shifted by about 20 nm (Fig. 1c).

Complexes **1**–**3** have a sharp singlet for the signals of the acetate protons in ^1H NMR spectra. All signals of pyridine protons in **1**–**3**, however, are broad singlet, possibly owing to the fast exchange of axial ligands with DMSO. The hydrogens of the picoline methyl of **1** are fully obscured by the methyl of DMSO solvent (δ 2.49 ppm). In the case of **2** and **3**, the methyl of DMSO was observed at δ 2.32 ppm and is partially overlapped with the picoline methyl. The ^{13}C NMR spectra of **1**–**3**, unfortunately, could not be detected because of the poor solubility in any solvents.

The structures of all three complexes were unambiguously determined by X-ray crystallography. Quality single crystals of **1**–**3**, suitable for X-ray analysis, were obtained by slow diffusion of an ethanol solution of picoline into an aqueous solution of $Rh_2(O_2CCH_3)_4$. Details of data collection and structure solution of these complexes are summarized in Table 1. The selected bond lengths and angles are listed in Tables 2–4.

The structure of **1** contains paddlewheel dirhodium units, as shown in Fig. 2, joined equatorially by four bidentate acetate ligands and two monodentate 2-picoline axial ligands bonded to the rhodium atoms by the nitrogen atom. Thus, each rhodium shows a slightly distorted octahedral environment having four equatorial positions occupied by the oxygen atoms of the acetate ligands; the axial sites are occupied by one nitrogen atom of 2-picoline and by the other Rh atom of the dirhodium unit. There is a

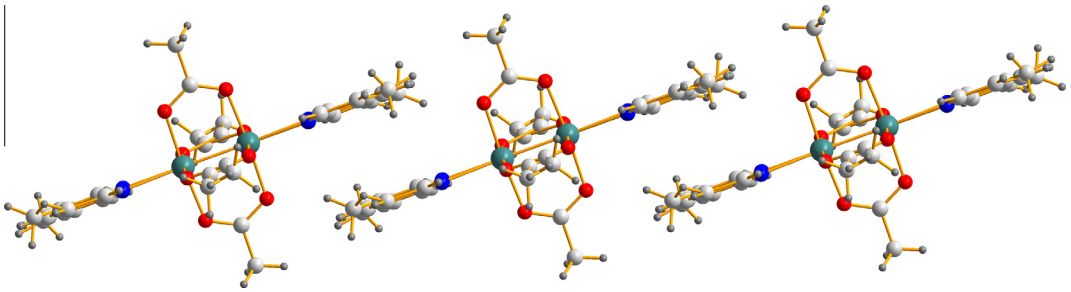

Fig. 5. The crystal packing of molecules **2**.

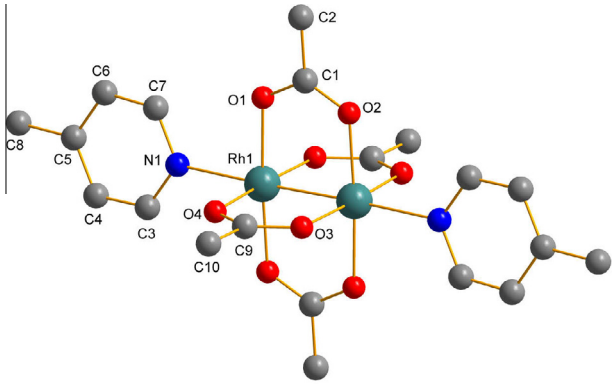

Fig. 6. A view of the molecule structure of **3** with the atomic labeling scheme. Hydrogen atoms were omitted for clarity.

crystallographic inversion center at the center of the Rh–Rh bond. The axial N–Rh–Rh–N chain is nearly linear with N–Rh–Rh angles of 176.42(7)°. The two groups of four equatorial oxygen atoms are almost perfectly eclipsed with respect to each other with a maximum O–Rh–Rh–O torsion angle of 1°. The ring atoms of the picoline are coplanar with a maximum deviation from the least-squares plane of 0.011 Å, and the methyl carbon (C5) lies 0.075(5) Å from this plane. The pyridine plane approximately bisects the acetate groups; it forms dihedral angles of 59.72(9)° and 30.33(9)° with the O1–O2–O1′–O2′ and O3–O4–O3′–O4′ planes of the bridging acetates, respectively.

The Rh–Rh bond length, 2.4121(5) Å, is slightly longer than that of $Rh_2(O_2CCH_3)_4(pyridine)_2$ (2.3963(2) Å) [25], whereas the Rh–N bond length (2.317(3) Å) shows a significantly longer than the value of $Rh_2(O_2CCH_3)_4(pyridine)_2$ (2.227(3) Å). The longer Rh–N bond found in **1** is obviously due to the steric repulsion between the 2-methyl groups and acetate oxygens, which have been reported for $Rh_2(O_2CCH_3)_4$ with axial pyridine derivatives having 2- or 6-methyl groups, $Rh_2(O_2CCH_3)_4$(2,6-dimethylpyridine)$_2$ (2.403(4) Å) [26], $Rh_2(O_2CCH_3)_4$(2-amino-6- ethylyridine)$_2$ (2.36(1) Å [27], bound to Rh atoms by the pyridine nitrogens) and $Rh_2(O_2CCH_3)_4$(2-acetylamino-6-methylpyridine)$_2$ (2.439(4) Å, bound to Rh atoms by the pyridine nitrogens). The Rh–N bond length increases in the following sequence of the ligand: pyridine < 2-picoline < 2-amino-6-methylpyridine < 2,6-dimethylpyridine < 2-acetylamino-6-methylpyridine. This is consistent with the steric effect caused by the substituents adjacent to the nitrogen donor. The Rh–Rh bond length also increases in the same order but is less affected (Table 5). The coordination of 2-picoline is assisted by two intramolecular C–H···O hydrogen bonds: C5···O4 = 3.044(5) Å and C5···O1 = 3.530(6) Å. The range of Rh–O distances extends from 2.039(2) to 2.051(2) Å, in agreement with those other dirhodium carboxylate compounds described in the literature [18].

The intermolecular C–H···O interactions play an important role in the structural stacking of **1** since stronger hydrogen bonding is absent [28]. As shown in Fig. 3a, a sheet is formed by the intermolecular C–H···O hydrogen bonds of C3···O3 (3.448(5) Å), C10···O2 (3.378(5) Å) and C10···O4 (3.500(6) Å). The sheets are further packed to afford three dimensions network (Fig. 3b).

The crystal structure of **2**, shown in Fig. 4, consists of centrosymmetric dinuclear dirhodium core with an inversion center located at the center of the Rh–Rh bond. The Rh–Rh distance (2.3837(4) Å) is 0.013 Å and 0.028 Å shorter than the values of $Rh_2(O_2CCH_3)_4(pyridine)_2$ [25] and **1**, respectively. Nevertheless, the Rh–N bond lengths (2.260(5), 2.252(5) Å) are significantly shorter than the value of **1** but slightly longer than that of $Rh_2(O_2CCH_3)_4(pyridine)_2$ (2.227(3) Å) [25]. The Rh–O bond lengths are similar to those of **1** and other dirhodium carboxylates [17,18]. The axial 3-picoline ligand and two carbon atoms (C7 and C8) of an acetate group are disordered, even though the data was collected at low temperature (100 K). The pyridine plane of 3-picoline almost parallels to the O1–O2–O1′–O2′ plane of the bridging acetates with a dihedral angle of 13.4(1)°.

As illustrated in Fig. 5, the molecules **2** are linked by π–π interactions between the neighboring pyridine rings, with which are parallel to each other at a distance of 3.585 Å and a centroids distance of 3.760 Å. Moreover, the intermolecular C–H···O interactions, formed between C10 and O3, C8 and O3, C8′ and O2 with *d*(C···O) of 3.452(4), 3.305(8) and 3.541(8) Å, respectively, also play an important role in the crystal packing of **2**.

The crystal structure of **3** is very similar to those of **1** and **2** except that the axial sites are occupied by 4-picoline instead of 2-picoline and 3-picoline for **1** and **2**, respectively (Fig. 6). The Rh–Rh distance is 2.4010(5) Å with the axial 4-picoline N atoms coordinates Rh at a distance of 2.247(3) Å. The Rh–N bond length is shorter than the value of **1** due to lack of steric repulsion adjacent to the 4-picoline nitrogen donor, but it still increase by 0.02 Å as compared to the value of $Rh_2(O_2CCH_3)_4(pyridine)_2$ (2.227(3) Å) [25]. It is interesting to note that both the Rh–Rh and Rh–N bond lengths of **3** are almost completely equal to the values of dirhodium tetraacetate 4-pyridinemethanol adduct (2.4030(7) and 2.243(3) Å for the Rh–Rh and Rh–N bond lengths, respectively) [29], even though the axial ligands vary from 4-

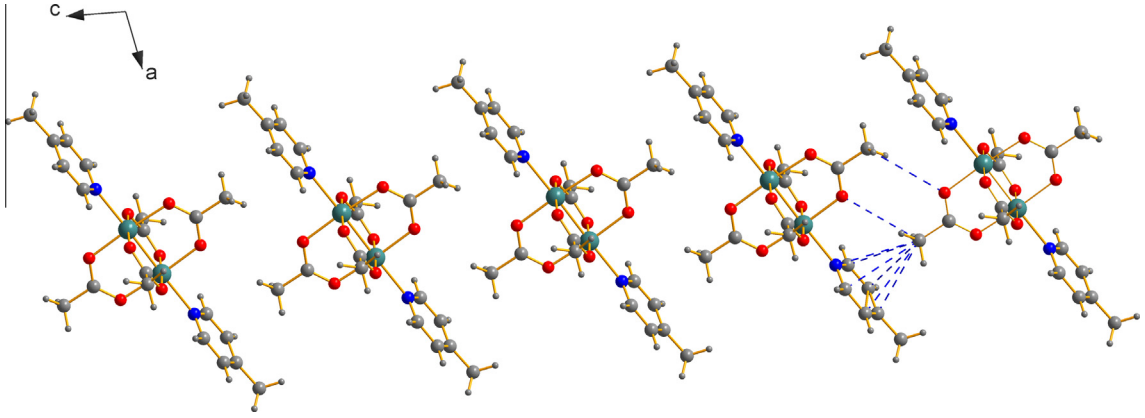

Fig. 7. A portion of the chain in **3** formed by C–H···π and C–H···O hydrogen (C10···*Cg* = 3.345 Å, *Cg* is the centroid of pyridine ring at (−*x*, −*y*, 1 − *z*); C2···O3^{i} = 3.601(5) Å and C2···O3^{ii} = 3.604(5) Å; symmetry code: (i) *x*, −0.5 − *y*, 0.5 + *z*; (ii) −*x*, −0.5 + *y*, 1.5 − *z*).

Table 6
Catalytic activity of **1**–**3** and dirhodium(II) tetraacetate.

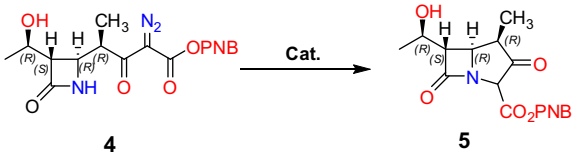

4 **5**

Catalyst	Axial ligands	Amount (mg)	Rh–Rh (Å)	Rh–N (Å)	Isolated yield
No catalyst	–	–	–	–	N.R.[b]
$Rh_2(O_2CCH_3)_4$	–	1	2.386(1)[a]	–	70 ± 2%
1	2-picoline	1	2.4121(5)	2.317(3)	40 ± 3%
2	3-picoline	1	2.3837(4)	2.260(5)	15 ± 3%
3	4-picoline	1	2.4010(5)	2.247(3)	20 ± 3%
$Rh_2(O_2CCH_3)_4$	–	5	2.386(1)[a]	–	72 ± 3%
1	2-picoline	5	2.4121(5)	2.317(3)	45 ± 4%
2	3-picoline	5	2.3837(4)	2.260(5)	17 ± 3%
3	4-picoline	5	2.4010(5)	2.247(3)	22 ± 3%
$Rh_2(O_2CCH_3)_4$	–	10	2.386(1)[a]	–	77 ± 3%
1	2-picoline	10	2.4121(5)	2.317(3)	48 ± 2%
2	3-picoline	10	2.3837(4)	2.260(5)	16 ± 4%
3	4-picoline	10	2.4010(5)	2.247(3)	25 ± 2%

[a] The value for $Rh_2(O_2CCH_3)_4(H_2O)_2$.
[b] N.R. means no reaction.

picoline to 4-pyridinemethanol, as seen in Table 5. The pyridine rings in 4-picoline are planar with deviations not greater than 0.01 Å, which nearly parallels to the O1–O2–O1′–O2′ plane of the bridging acetates with a dihedral angle of 7.7(1)°.

The crystal structure of **3** contains an intermolecular C–H···π interactions in which atom C10 interact with the nearest pyridine rings of 4-picoline at a distance of 3.345 Å from the centroid of the pyridine rings. This interaction links the molecules **3** to form an infinite chain, as seen in Fig. 7. The chain is further stabilized by a weak C–H···O hydrogen bond formed between atoms C10 and O3 at a distance of 3.784(5) Å. These chains form the same three dimensions network as that of **1**, assisted by two intermolecular C–H···O hydrogen bonds (C2···O3^{i} = 3.601(5) Å and C2···O3^{ii} = 3.604(5) Å; symmetry code: (i) x, $-0.5-y$, $0.5+z$; (ii) $-x$, $-0.5+y$, $1.5-z$).

Dirhodium(II) complexes are exceptionally active catalysts for the decomposition of diazo compounds to form rhodium carbenoids, which undergo a number of highly selective reactions such as cyclopropanation, carbon-hydrogen insertion, ylide generation, and aromatic cycloaddition [1,2,30–32]. Inspiring by their unique catalysis, much attentions has focused on tuning their catalyst properties by modification of the bridge ligand structure. The axial ligand, however, had long been considered to have a less important or negative role in catalysis, since it was observed that dirhodium(II) tetracarboxylates were more efficient in solvents with poor coordinative capabilities than in medium to strong coordinative solvents. In other words, medium to strong donor ligands can partially or totally inhibit the catalysis. Therefore, less work was done about the catalysis of dirhodium(II) tetracarboxylates adducts over a long time [1,2]. This concept is changing, and several studies have proven that the axial ligand modification also is a valuable and simple strategy to prepare new catalysts of dirhodium(II) tetracarboxylates [33]. In this context, we evaluated the catalytic activity of **1**–**3** for the preparation of a Meropenem intermediate (**5**, Table 6). Compounds **4** and **5** were characterized by NMR (Fig. 8), specific rotation and ESI-MS, being in good agreement with the assigned structures.

As can be seen from Table 6 (line 1), without a catalyst, the reaction is not going to happen. However, under different amount of the catalyst, there is litter difference in isolated yields, such as for complex **1**, the yields are 40% (using 1 mg), 45% (using 5 mg) and 48% (using 10 mg), respectively. For complex **2**, the yields are 15% (using 1 mg), 17% (using 5 mg) and 16% (using 10 mg), respectively. And for complex **3**, the yields are 20% (using 1 mg), 22% (using 5 mg) and 25% (using 10 mg), respectively. The possible reason is that the poor solubilities of **1**–**3** have made them saturation in the reaction system under different amount of the catalyst. It is noted that all the isolated yields of the evaluation reaction for **1**–**3** are significantly lower than the value of dirhodium(II)

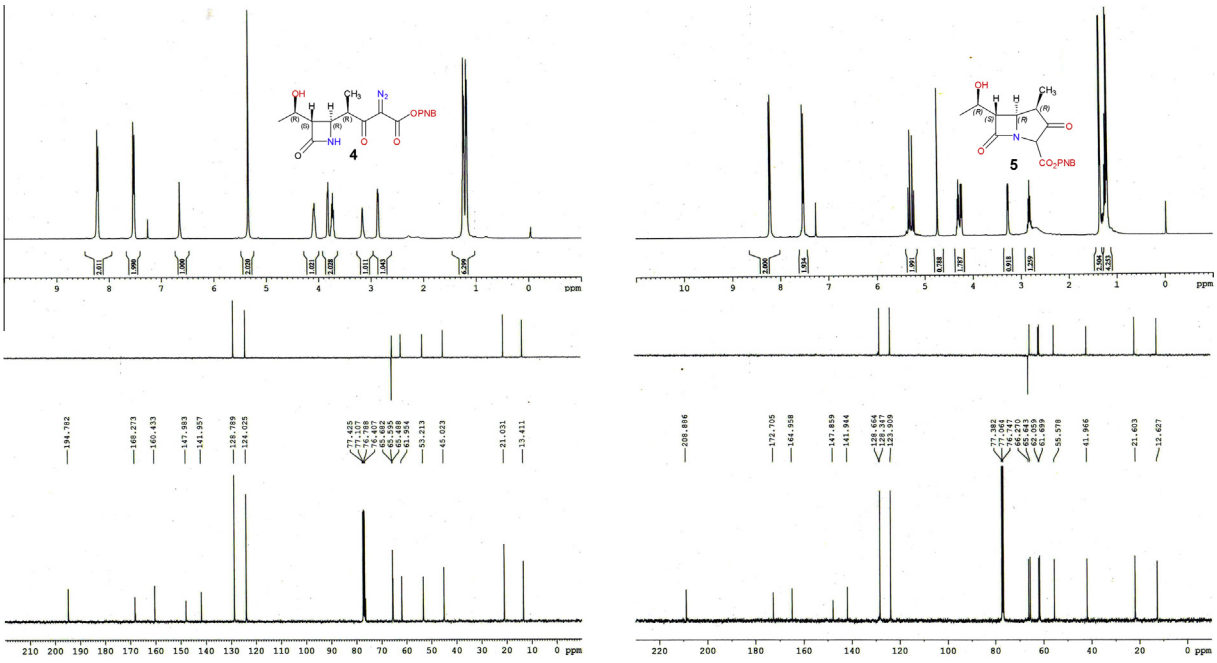

Fig. 8. The ^{1}H NMR and ^{13}C NMR spectrums of compounds **4** and **5**.

tetraacetate (Table 6). The main reason may be that the axial sites of dirhodium(II) tetraacetate are occupied by the strong donor ligands picoline, which makes it difficult for the axial ligands to be displaced from the catalysts, and then limits the chance of the rhodium atom contact with the reaction substrate. In additional, it is worthy to note that the most efficient complex **1** has the longest Rh–N bond distance in the three adducts (Table 6). This can be explained by that the longer Rh–N bond distance of **1** makes its axial ligands leave readily and then more better catalytic activity is observed, which is also supported by the UV–Vis analysis that **1** is more easy to form solvation molecule ($Rh_2(O_2CCH_3)_4(solvent)_2$) than **2** and **3**. Therefore, it can be concluded that the catalytic activity of **1**–**3** are related to the Rh–N bond lengths, and it is still possible to tune the catalytic activity of $Rh_2(O_2CCH_3)_4$ by changing its axial ligands.

4. Conclusion

In summary, we have synthesized three adducts of dirhodium(II) tetraacetate with picoline as the axial ligands and characterized them by elemental analysis, ESI^+-MS, FT-IR and ^1H NMR. Moreover, all the three complexes were unambiguously determined by single-crystal X-ray structural analysis. All picoline ligands coordinate to the axial sites of dirhodium(II) tetraacetate via the nitrogen atoms, and in complex **1**, the coordination of 2-picoline is further assisted by two intramolecular C–H···O hydrogen bonds. It is interesting to note that the intermolecular C–H···O interactions also play an important role in the structural stacking of **1**–**3** due to the absence of strong hydrogen bonding. An evaluation reaction for the preparation of Meropenem key intermediate has showed that their catalytic activity was inhibited by the axial ligands. But the results suggest that the catalytic activity of $Rh_2(O_2CCH_3)_4$ can be tuned by changing its axial ligands. Further research to tune the catalytic property of dirhodium(II) tetraacetate is on-going.

Acknowledgements

This work was financially supported by Science and Technology Development Program of Yunnan Province and Ministry of Science and Technology of PR China (No: 2013B019, 2012EG115008).

Appendix A. Supplementary data

CCDC 1022719, 1022720 and 1022720 contains the supplementary crystallographic data for Complexes **1**–**3**. These data can be obtained free of charge from The Cambridge Crystallographic Data Centre via www.ccdc.cam.ac.uk/data_request/cif. Supplementary data associated with this article can be found, in the online version, at http://dx.doi.org/10.1016/j.ica.2015.05.017. These data include MOL files and InChiKeys of the most important compounds described in this article.

References

[1] J. Hansen, H.M.L. Davies, Coord. Chem. Rev. 252 (2008) 545.
[2] M.P. Doyle, J. Org. Chem. 71 (2006) 9253.
[3] M.P. Doyle, R. Duffy, M. Ratnikov, L. Zhou, Chem. Rev. 110 (2010) 704.
[4] H. Choi, M.P. Doyle, Chem. Commun. (2007) 745.
[5] M. Barberis, J. Perez-Prieto, K. Herbst, P. Lahuerta, Organometallics 21 (2002) 1667.
[6] M.N. Sokolov, S.A. Adonin, E.V. Peresypkina, P.A. Abramov, A.I. Smolentsev, D.I. Potemkin, P.V. Snytnikov, V.P. Fedin, Inorg. Chim. Acta 394 (2013) 656.
[7] J.M. Asara, J.S. Hess, E. Lozada, K.R. Dunbar, J. Allison, J. Am. Chem. Soc. 122 (2000) 8.
[8] H.T. Chifotides, J.S. Hess, A.M. Angeles-Boza, J.R. Galán-Mascarós, K. Sorasaenee, K.R. Dunbar, Dalton Trans. (2003) 4426.
[9] R.F.M. Frade, N.R. Candeias, C.M.M. Duarte, V. André, M.T. Duarte, P.M.P. Gois, C.A.M. Afonso, Bioorg. Med. Chem. Lett. 20 (2010) 3413.
[10] M. Ćwikowska, F.P. Pruchnik, R. Starosta, H. Chojnacki, A. Wilczok, S. Ułaszewski, Inorg. Chim. Acta 363 (2010) 2401.
[11] H.T. Chifotides, P.K.-L. Fu, K.R. Dunbar, C. Turro, Inorg. Chem. 43 (2004) 1175.
[12] P.K.-L. Fu, P.M. Bradley, C. Turro, Inorg. Chem. 40 (2001) 2476.
[13] M. Angeles-Boza, H.T. Chifotides, J.D. Aguirre, A. Chouai, P.K.-L. Fu, K.R. Dunbar, C. Turro, J. Med. Chem. 49 (2006) 6841.
[14] R.P. Bonar-Law, T.D. McGrath, N. Singh, J.F. Bickley, A. Steiner, Chem. Commun. (1999) 2457.
[15] J.F. Bickley, R.P. Bonar-Law, C. Femoni, E.J. MacLean, A. Steiner, S.J. Teat, J. Chem. Soc., Dalton Trans. (2000) 4025.
[16] F.A. Cotton, C. Lin, C.A. Murillo, Acc. Chem. Res. 34 (2001) 759.
[17] F.A. Cotton, C.A. Murillo, R.A. Walton, Multiple Bonds between Metal Atoms, 3rd ed., Springer-Science and Business Media Inc., New York, 2005.
[18] E.B. Boyar, S.D. Robinson, Coord. Chem. Rev. 50 (1983) 109.
[19] G.A. Rempel, P. Legzdins, H. Smith, G. Wilkinson, Inorg. Synth. 13 (1972) 90.
[20] G.M. Sheldrick, Acta Crystallogr. A 64 (2008) 112.
[21] D.H. Shih, F. Baker, L. Cama, B.G. Chrisrtensen, Heterocycles 21 (1984) 29.
[22] L. Zhang, Y. Liu, L. Liu, S.H. Ni, J. Li, Chin. J. Pharm. 41 (2010) 891.
[23] K. Nakamoto, Infrared and Raman Spectra of Inorganic and Coordination Compounds, 4th ed., Wiley Interscience, New York, 1986.
[24] Q.-S. Ye, X.-Z. Chen, M.-J. Xie, W.-P. Liu, J.-L. Chen, Z.-F. Pan, Transition Met. Chem. 35 (2010) 585.
[25] Y.B. Koh, G.G. Christoph, Inorg. Chem. 17 (1978) 2590.
[26] K. Aoki, M. Inaba, S. Teratani, H. Yamazaki, Y. Miyashita, Inorg. Chem. 33 (1994) 3018.
[27] H. Kitamura, T. Ozawa, K. Jitsukawa, H. Masuda, Y. Aoyama, H. Einaga, Inorg. Chem. 39 (2000) 3294.
[28] G.R. Desiraju, Acc. Chem. Res. 29 (1996) 441.
[29] Q.-S. Ye, J.-L. Chen, M.-J. Xie, W.-P. Liu, S.-Y. Yang, Z. Kristallogr, NCS 226 (2011) 147.
[30] A. Padwa, S.F. Hornbuckle, Chem. Rev. 91 (1991) 263.
[31] M.P. Doyle, M.S. Shanklin, H.Q. Pho, Tetrahedron Lett. 29 (1988) 2639.
[32] M. Mikołajczyk, R. Zurawiński, P. Kiełbasiński, Tetrahedron Lett. 30 (1989) 1143.
[33] A.F. Trindade, J.A.S. Coelho, C.A.M. Afonso, L.F. Veiros, P.M.P. Gois, ACS Catal. 2 (2012) 370.